

# Contrasting response of European forest and grassland energy exchange to heatwaves

Adriaan J. Teuling<sup>1,2\*</sup>, Sonia I. Seneviratne<sup>1\*</sup>, Reto Stöckli<sup>3</sup>, Markus Reichstein<sup>4</sup>, Eddy Moors<sup>5</sup>, Philippe Ciais<sup>6</sup>, Sebastiaan Luyssaert<sup>6</sup>, Bart van den Hurk<sup>7</sup>, Christof Ammann<sup>8</sup>, Christian Bernhofer<sup>9</sup>, Ebba Dellwik<sup>10</sup>, Damiano Gianelle<sup>11</sup>, Bert Gielen<sup>12</sup>, Thomas Grünwald<sup>9</sup>, Katja Klumpp<sup>13</sup>, Leonardo Montagnani<sup>14,15</sup>, Christine Moureaux<sup>16</sup>, Matteo Sottocornola<sup>11</sup> and Georg Wohlfahrt<sup>17</sup>

**Recent European heatwaves have raised interest in the impact of land cover conditions on temperature extremes. At present, it is believed that such extremes are enhanced by stronger surface heating of the atmosphere, when soil moisture content is below average. However, the impact of land cover on the exchange of water and energy and the interaction of this exchange with the soil water balance during heatwaves is largely unknown. Here we analyse observations from an extensive network of flux towers in Europe that reveal a difference between the temporal responses of forest and grassland ecosystems during heatwaves. We find that initially, surface heating is twice as high over forest than over grassland. Over grass, heating is suppressed by increased evaporation in response to increased solar radiation and temperature. Ultimately, however, this process accelerates soil moisture depletion and induces a critical shift in the regional climate system that leads to increased heating. We propose that this mechanism may explain the extreme temperatures in August 2003. We conclude that the conservative water use of forest contributes to increased temperatures in the short term, but mitigates the impact of the most extreme heat and/or long-lasting events.**

Climate extremes, such as prolonged periods of above-average high temperatures, have a large societal and economic impact. In Central and Western Europe, both average summer temperatures and heatwave occurrence are projected to increase in the coming decades<sup>1–4</sup>, associated with a transition towards a dryer summer climate regime<sup>2</sup>. Trends in past decades are consistent with these projections<sup>5</sup>. Large-scale, record-breaking summer heatwaves occurred recently in 2003 (refs 1,6–8) and 2006 (ref. 9), associated with widespread ecosystem damage and crop failures, increased human mortality and water shortages<sup>1,7,10–12</sup>. European heatwaves are favoured by two atmospheric circulation patterns<sup>13</sup>: a deep anomalous trough covering the North Atlantic (June 2003; ref. 13), and an Omega blocking situation with an extensive high located over Northern Europe (August 2003, ref. 13; July 2006, ref. 9; see Supplementary Fig. S1). Model simulations and heat budget analyses suggest that the warm conditions associated with these circulation patterns can be amplified by reduced evaporative cooling because of soil moisture depletion<sup>2,6,11,14</sup>. However, the relation between land cover and the temporal dynamics of evapotranspiration (hereafter ET) and its impact on temperature during heatwave days (HWDs, see the Methods section) remain to be quantified.

Land-use-related variations in surface exchanges have the potential to impact local climate<sup>15,16</sup>, but the direction of this effect on global climate is uncertain<sup>17–20</sup>. It has been suggested that short herbaceous (perennial) vegetation and forest respond differently to conditions typical for HWDs (refs 8,21). Although forest ET generally exceeds that of grassland on annual timescales<sup>22</sup>, guard cells around stomata may have evolved different strategies to cope with drought conditions that often accompany heatwaves<sup>23</sup>. The strong regulation of stomatal opening in response to radiation, temperature and vapour pressure deficit<sup>21,24–26</sup> and the larger rooting depth<sup>27</sup> probably contribute to the conservative character and persistence of forest ET (refs 28,29). Thus, whereas evaporative cooling over grassland might exceed that over forest at times of ample soil moisture<sup>17,30</sup>, the reverse is likely to occur under low soil moisture conditions<sup>8,31,32</sup>. As a result, it is uncertain whether most heating during HWDs takes place over forest or grassland<sup>8,30</sup>.

## Energy exchange under normal summer conditions

We first analyse the flux partitioning in central-western Europe under normal summer conditions on the basis of observations from a network of eddy covariance flux towers<sup>33</sup>. We selected only towers where temperature and precipitation fall within the

<sup>1</sup>Institute for Atmospheric and Climate Science, ETH Zurich, 8092 Zurich, Switzerland, <sup>2</sup>Hydrology and Quantitative Water Management Group, Wageningen University, 6709PA Wageningen, The Netherlands, <sup>3</sup>Climate Science, Climate Analysis, MeteoSwiss, 8044 Zurich, Switzerland, <sup>4</sup>Max-Planck Institute for Biogeochemistry, 07745 Jena, Germany, <sup>5</sup>Alterra, 6708PB Wageningen, The Netherlands, <sup>6</sup>Laboratoire des Sciences du Climat et de l'Environnement, LSCE, 91191 Gif-sur-Yvette, France, <sup>7</sup>KNMI, 3730AE De Bilt, The Netherlands, <sup>8</sup>Agroscope ART, 8046 Zurich, Switzerland, <sup>9</sup>Institute of Hydrology and Meteorology, TU Dresden, 01062 Dresden, Germany, <sup>10</sup>Risø National Laboratory for Sustainable Energy, Technical University of Denmark, 4000 Roskilde, Denmark, <sup>11</sup>IASMA Research and Innovation Centre, Fondazione E. Mach, Environment and Natural Resources Area, 38040 Trento, Italy, <sup>12</sup>Department of Biology, University of Antwerp, 2610 Wilrijk, Belgium, <sup>13</sup>INRA, Grassland Ecosystem Research (UREP), 63100 Clermont-Ferrand, France, <sup>14</sup>Forest Services and Agency for the Environment, 39100 Bolzano, Italy, <sup>15</sup>Faculty of Sciences and Technology, University of Bozen-Bolzano, 39100 Bolzano, Italy, <sup>16</sup>Gembloux Agro-Bio Tech, University of Liège, 5030 Gembloux, Belgium, <sup>17</sup>Institute of Ecology, University of Innsbruck, 6020 Innsbruck, Austria. \*e-mail: ryan.teuling@wur.nl; sonia.seneviratne@env.ethz.ch.

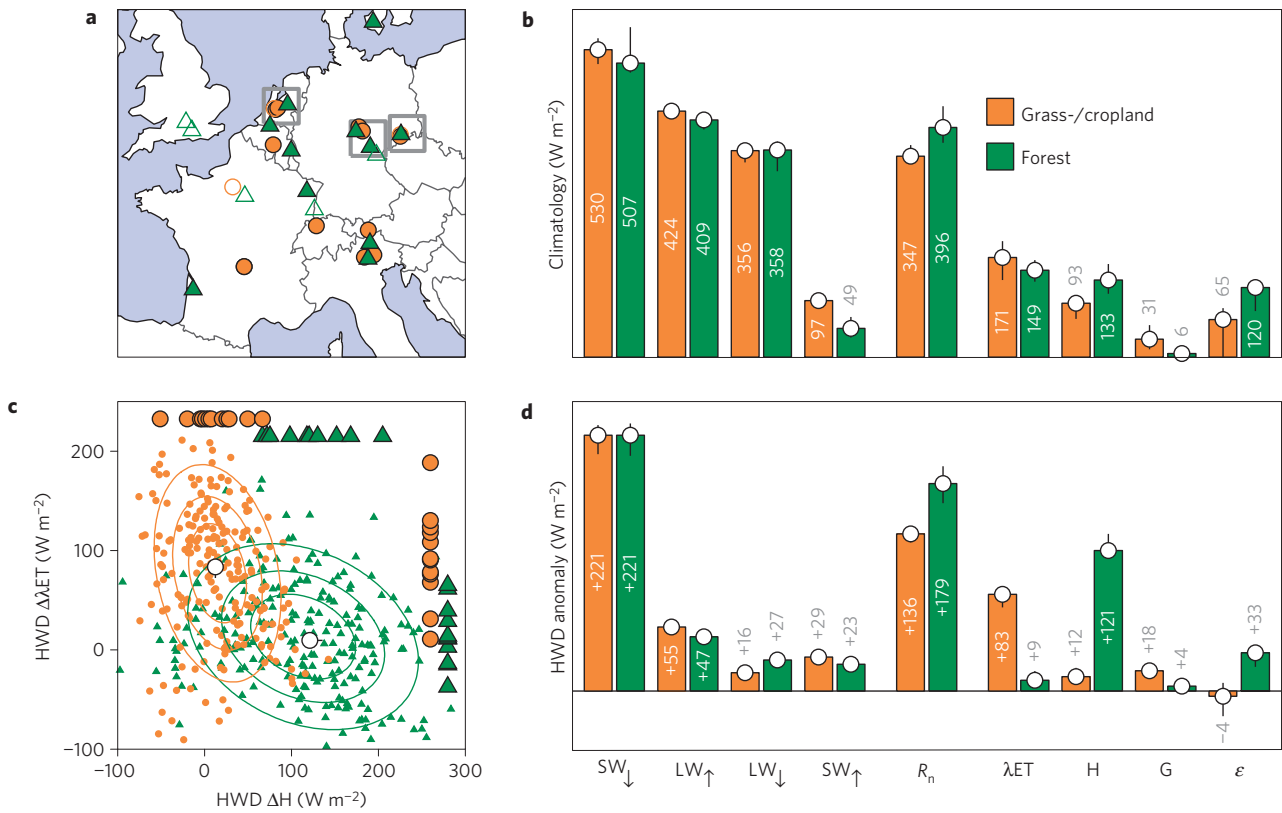


**Figure 1 | Radiation and energy exchange over forest and grassland.** The balance of incoming (downarrow) and outgoing (uparrow) short-wave (SW) and long-wave (LW) radiation determines the net radiation ( $R_n$ ) available for latent ( $\lambda$ ET), sensible (H) and ground (G) heat fluxes. The residual ( $\epsilon = R_n - \lambda$ ET - H - G) encompasses both missing balance terms and bias. **a**, Location of flux towers. The open markers indicate multi-year sites without HWD observations. Orange circles indicate grass-/cropland; green triangles indicate forest. **b**, Flux climatologies. **c**, HWD sensible and latent heat flux anomalies  $\Delta H$  and  $\Delta \lambda$ ET with single-component Gaussian density contours and site medians. **d**, HWD anomalies. The vertical lines indicate 95% confidence limits for medians determined by bootstrapping.

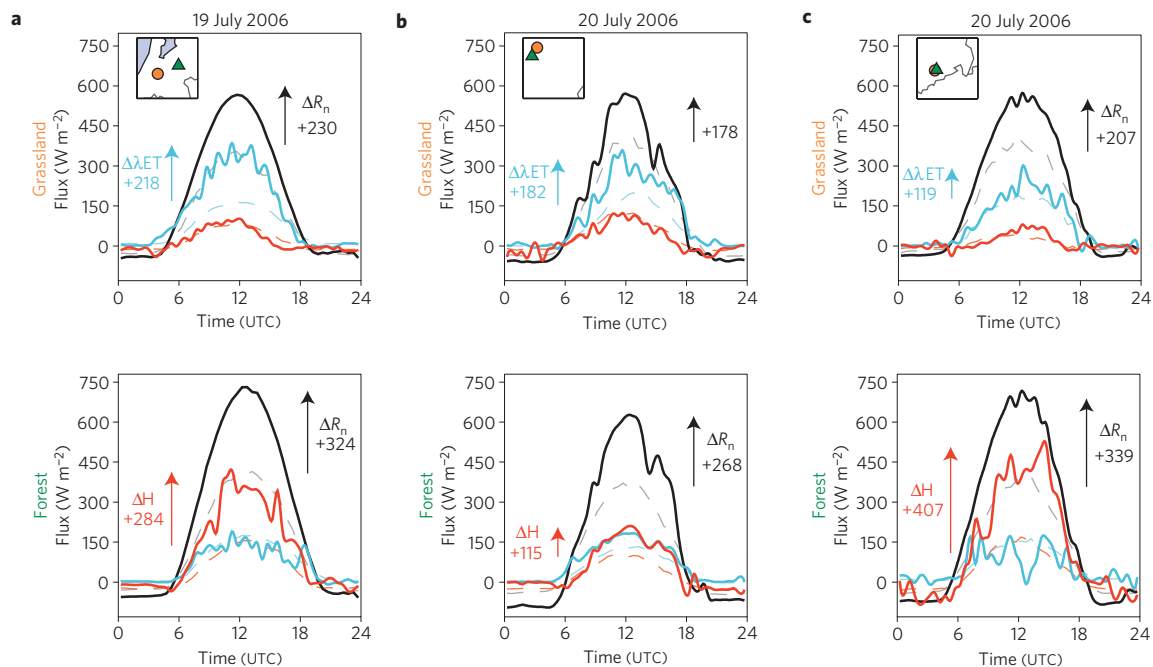


**Figure 2 | Energy exchanges at the peak of the July 2006 heatwave for neighbouring flux towers over forest and grassland.** **a**, Cabauw and Loobos (distance 60 km). **b**, Mehrstedt and Hainich (distance 26 km). **c**, Grillenburg and Tharandt (distance 4 km). The solid lines indicate HWD values; the dashed lines indicate the baseline conditions in a normal year. Black: net radiation ( $R_n$ ), blue: latent heat flux ( $\lambda$ ET), red: sensible heat flux (H). The arrows indicate maximum anomalies  $\Delta$  for  $\lambda$ ET (grassland sites, upper panels), H (forest sites, lower panels) and  $R_n$ . See Fig. 1 for location of map insets.

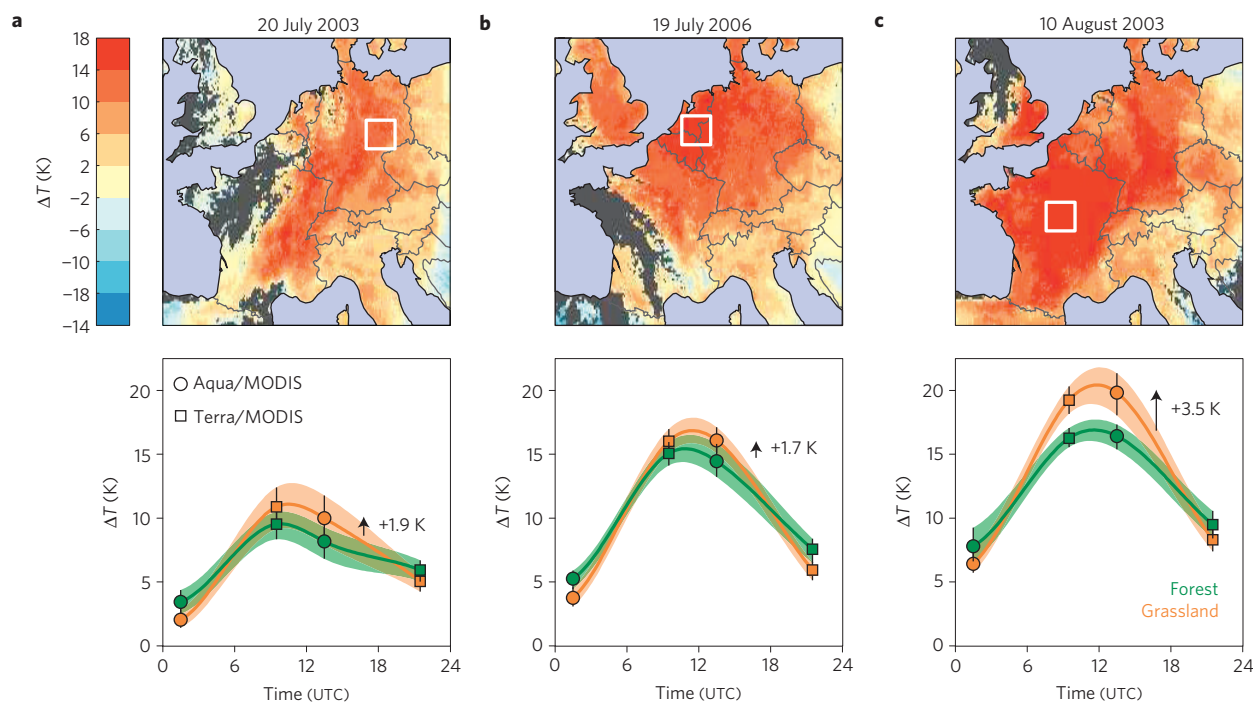


**Figure 3 | Impact of land cover on local LST anomalies during heatwaves. a**, Onset of heatwave (July 2003). **b**, Normal heatwave (July 2006). **c**, Extreme heatwave (August 2003). Upper panels: daytime LST anomaly distribution (Terra/MODIS,  $0.1^\circ$  resolution). The dark shading indicates cloud cover. Lower panels: evolution of median temperature anomalies for selected regions ( $1.4^\circ \times 2.4^\circ$ ) on the basis of the high-resolution ( $30''$ ) data. The vertical lines indicate 25th and 75th percentiles. Data have been observed with MODIS aboard the Terra (squares, overpass 9:30/21:30 h local solar time) and Aqua (circles, overpass 01:30/13:30 h) satellites. Splines were used for interpolation.

range of maritime temperate or hemiboreal climates and where flux climatologies could be estimated from at least two years of observations (Fig. 1a, see the Methods section and Supplementary Table S1 for site characteristics and references). The towers sample the actual land-use distribution; hence, our results include the possible impact of co-varying (sub)surface characteristics. The summer (June–August) climatology is calculated over all available years in the period 1997–2008 (but excluding 2003 and July 2006). We focus on a four-hour period (9:00–13:00 UTC) during which heating at the land surface is maximum and controls the magnitude of the diurnal temperature peak (note that there is a phase shift between the diurnal cycles of heating and temperature). Figure 1b shows the main radiation and energy balance terms for grass-/cropland and forest sites. Median values are shown to minimize the impact of outliers. The terms do not balance owing to different data gaps in the radiation and flux terms. Large differences exist in reflected short-wave and net radiation ( $48$  and  $49 \text{ W m}^{-2}$ , respectively, with forest absorbing more incoming short-wave radiation<sup>31</sup>). Forest emits  $40 \text{ W m}^{-2}$  more sensible heat (H). The lack of measured energy balance closure is larger over forest (30%) than grassland (19%). This range is consistent with previous findings<sup>31,34,35</sup> and is primarily caused by underestimation of heat exchange by the eddy covariance technique<sup>36–38</sup>. The difference in closure ( $55 \text{ W m}^{-2}$ ) may be partly attributed to larger heat storage in forest between the land surface and the eddy covariance sensor<sup>31,35,39</sup>, which is implicitly included in the closure residual term ( $\epsilon$ ), as well as greater flow distortion errors on the sonic anemometer vertical velocity<sup>38,40</sup>.

### Energy exchange under heatwave conditions

During HWDs, the measured energy balance residual improves to 27% over forest and 13% over grassland. This improvement is consistent with expected smaller instrumental errors on evaporation during dry conditions<sup>36</sup>. Large positive incoming radiation anomalies ( $+221 \text{ W m}^{-2}$ ) reflect low cloud cover typical for

anticyclones<sup>6,13</sup>. The increase in available energy is larger over forest than over grassland, mainly owing to changes in long-wave radiation. Albedo changes have limited impact<sup>41</sup>. The change in partitioning over forest and grassland diverges strongly (Fig. 1c,d). During the transition from wet to dry soil moisture conditions typical for HWDs, different stages can be distinguished, reflecting the nonlinear relationship between soil moisture and ET (refs 24, 31,42,43): (1) stage I drying during which ET is independent of soil moisture<sup>31,44</sup>, (2) stage II drying during which ET becomes self-limiting<sup>29,44</sup> and (3) stage III during which ET becomes negligible<sup>31</sup>. Note that the latent heat flux  $\lambda ET$  and ET relate through the latent heat of vaporization  $\lambda$ . Our analysis reveals that the additional energy over grassland ( $+136 \text{ W m}^{-2}$ ) is primarily used for evaporation of water ( $+83 \text{ W m}^{-2}$ ), rather than increasing sensible heating ( $+12 \text{ W m}^{-2}$ ). The average decrease in Bowen ratio (the ratio  $H/\lambda ET$  between sensible and latent heat flux) from 0.54 to 0.41 indicates stage I rather than stage II drying<sup>44</sup>. In contrast, forest maintains similar  $\lambda ET$  ( $+9 \text{ W m}^{-2}$ ) but uses the additional energy ( $+179 \text{ W m}^{-2}$ ) to effectively double H ( $+121 \text{ W m}^{-2}$ ), thereby increasing the Bowen ratio from 0.89 to 1.60. The median HWD anomalies for H and  $\lambda ET$  both differ significantly between forest ( $n = 231$ ) and grass-/cropland ( $n = 210$ ) sites (two-sided Wilcoxon rank sum test,  $p < 0.001$ ).

These results are consistent with previous findings around the German Hartheim site under cloudless conditions and ample supply of soil moisture<sup>30</sup>. Given the deeper roots of forest ecosystems<sup>27,45,46</sup>, this increase should be attributed to the differential response of stomatal opening to radiation and atmospheric boundary layer feedbacks with temperature and humidity<sup>21,24,25</sup> (see Supplementary Fig. S2), rather than soil moisture. In addition, the rough surface of forest canopies provides a more efficient turbulent heat exchange with the boundary layer<sup>20,21,30,47</sup>, such that convective cooling relaxes the need for strong evaporative cooling during HWD conditions. The energy balance constraint is reflected in the

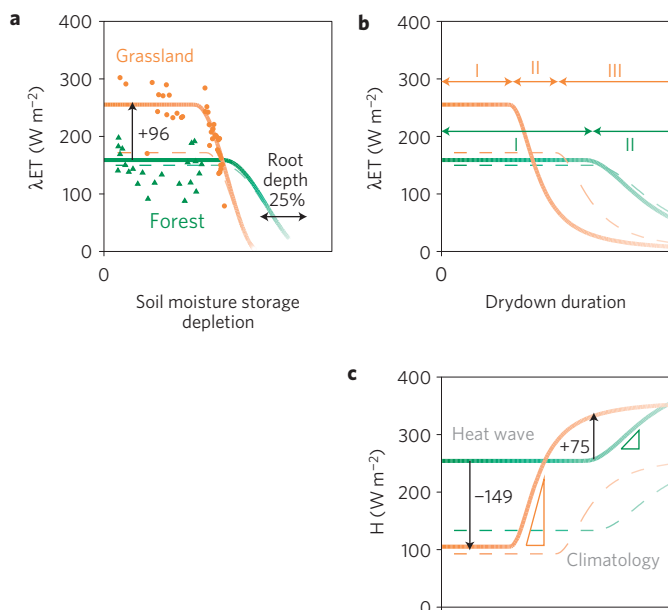


**Figure 4 | Conceptual model for flux evolution over grassland and forest during drydown.** See the Methods section for details. **a**, Relation between soil moisture storage depletion and midday latent heat flux  $\lambda\text{ET}$ . **b**, Temporal evolution of  $\lambda\text{ET}$ . **c**, Temporal evolution of sensible heat flux  $H$ . Values for  $\lambda\text{ET}$  and  $H$  during stage I drying are taken from Fig. 1, with dashed lines corresponding to the hypothetical situation of drydown under average conditions and thick lines corresponding to climatologies plus HWD anomalies. The points indicate independent observations of  $\lambda\text{ET}$  and soil moisture for Oensingen (grassland) and Wetzstein (forest) for HWDs in 2003 and July 2006.

distinct clustering of HWD anomalies of  $H$  and  $\lambda\text{ET}$  for forest and grassland sites, and also in the median HWD anomalies for the individual stations (Fig. 1c and Supplementary Fig. S3). The scatter originates from random errors, daily variation in atmospheric conditions during HWDs and from errors in estimating the baseline condition from limited data (contribution 20–30  $\text{W m}^{-2}$ , see the Methods section and Supplementary Fig. S4).

The contrasting Bowen ratio response can lead to marked energy budget differences at small spatial scales with a common atmospheric forcing. Figure 2 shows the diurnal cycle of the key elements of the land energy budget at the peak of the 2006 heatwave for three pairs of neighbouring flux towers over forest and grassland. Although all sites experienced nearly cloud-free conditions, the maximum net radiation anomaly over the forested sites exceeds that of the grassland sites by 90–132  $\text{W m}^{-2}$ . Combined with the Bowen ratio response, this results in a situation where the maximum heating of the atmosphere is up to four times larger at the forested sites than at grassland sites (420 versus 100  $\text{W m}^{-2}$ , respectively, at the Dutch Cabauw and Loobos sites). Thus, forests literally seem to be ‘hot-spots’ during the analysed summer heatwave conditions in Europe. In spite of the low soil moisture levels at all sites (see Supplementary Fig. S5), the strong positive response of  $\lambda\text{ET}$  over grassland indicates stage I drying. Unfortunately, no flux observations are available over short vegetation in the low parts of Central France during the August 2003 extreme where large soil moisture depletion probably induced stage II drying<sup>8,9,48</sup>.

### Impact on land surface temperature

To diagnose flux partitioning across heatwave scenes of various intensities, including the August 2003 extreme, we employ satellite observations of land surface temperature (LST). The Moderate Resolution Imaging Spectroradiometer (MODIS) aboard the Terra and

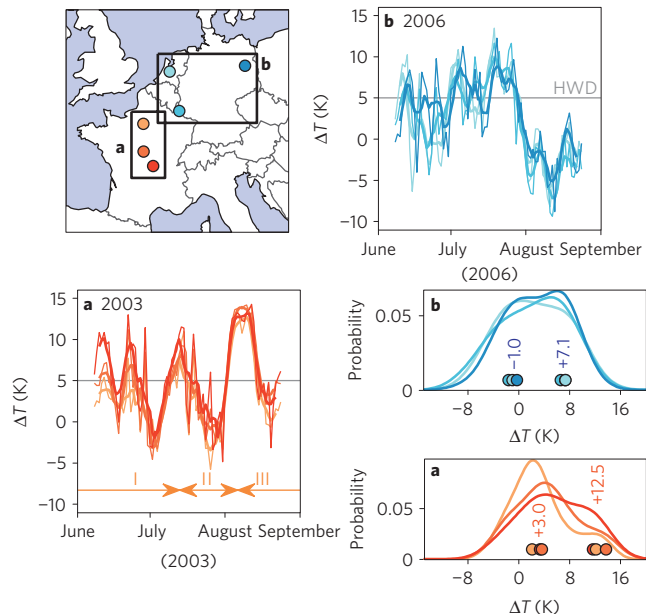


**Figure 5 | Screen-level daily maximum temperature anomaly evolution and distribution during heatwaves.** Observations are made over grassland at meteorological stations. **a**, Paris, Bourges, Vichy (2003). **b**, De Bilt, Luxembourg, Berlin (2006). The thick lines represent five-day moving averages. The circles indicate the means of individual components obtained by fitting a mixture of two Gaussian densities. The data are taken from the European Climate Assessment and Dataset. Temperature anomalies over forest will differ less between 2003 and 2006 than those measured over grassland (Fig. 3). The arrows in the bottom left subplot **a** indicate the possible drydown stages during the summer of 2003.

Aqua platforms provides sufficient spatial detail (30'') to distinguish between main land-use variations; moreover its records are long enough to determine anomalies (see the Methods section). Figure 3 shows the distribution of LST anomalies for pixels consisting predominantly (>67%) of grassland or forest during three HWD scenes. The scenes have been selected on the basis of land cover mixture, absence of cloud cover and absence of strong regional LST gradients. The strong diurnal cycle of the LST anomalies confirms the key role of daytime heating on maximum temperatures. Whereas for the July 2003 and July 2006 scenes the LST anomalies for grassland and forest are similar (Fig. 3a,b), they deviate during the peak of the August 2003 heatwave in Central France (Fig. 3c). The higher daytime anomalies over grassland are consistent with previous findings<sup>8</sup> and indicate a phase transition over grassland in this region towards a state with increased heating and temperatures. Note that Fig. 3a,b reflects stage I drying whereas the increased temperature anomalies in Fig. 3c indicate stage II/III drying over grassland.

### Preferred states in heating and air temperature

We explore the potential for a phase transition during extended heatwave duration with a conceptual model that includes differences observed during stage I drying (Fig. 1) and is consistent with independent observations of stage II and III drying (see the Methods section). Figure 4a illustrates the typical nonlinear relationships between soil moisture storage and ET, with a sharp drop in ET at low storage<sup>24,42</sup>. The nonlinearity is confirmed by observations from the Swiss Oensingen grassland site, one of the sites where the impact of the August 2003 heatwave was strongest, with  $\lambda\text{ET}$  dropping to 31% of the HWD median at low soil moisture. Soil moisture depletion at the German Wetzstein forest site was not sufficient to induce sensitivity to soil moisture. Figure 4b,c, shows the effect of the nonlinearity on the dynamics of  $\lambda\text{ET}$  and  $H$  during a hypothetical continuous

drydown. For grassland, increased  $\lambda ET$  combines with the effect of shallower roots to expedite the onset of stage II drying to occur within the duration of the 2003 extreme as shown by the Oensingen data<sup>1,6</sup>. The onset of stage II drying can be regarded as a critical transition during which the system rapidly changes from a metastable state (stage I) characterized by suppressed sensible heating to a stable state in which heating triples and becomes limited only by the available energy and ET is negligible (stage III). In the absence of rain, this transition can occur in approximately a week's time<sup>29</sup>. It represents a crossing point where grassland surpasses forest as the main source of heating for the atmosphere. Over forest, H is less dynamic and almost insensitive to changes in  $\lambda ET$  (ref. 49). A second crossing point exists because of the larger net radiation over forest.

The existence of two preferred states in the sensible heat flux can induce different modes in the regional temperature distribution. Figure 5 shows the evolution and distribution of the daily maximum temperature anomalies at six meteorological stations in the centre of the 2003 and 2006 heatwaves. In 2003, the extreme temperatures in France (exceeding 40 °C) were reached only in August after a dry and warm summer with soil moisture depletion exceeding 2006 levels<sup>48,50</sup>. In 2003, dry conditions already started in May<sup>48</sup>, whereas in 2006 the drought period was restricted to July and too short to cause widespread stage II drying. Although the monthly average daily maximum temperature anomaly in July 2006 exceeded that of August 2003 (ref. 9), maximum temperature anomalies on individual HWDs were smaller. To identify the preferred modes we fit a mixture of two Gaussian densities to the daily maximum temperature anomalies. In both cases the modes can be attributed to climatological ( $\approx 0$  K) and heatwave conditions ( $> +5$  K). The average heatwave mode for 2003 exceeds that of 2006 (+12.5 K versus +7.1 K, respectively), which is consistent with the phase transition induced by the larger soil moisture depletion in 2003.

The most striking result of our study is that initially, the increase in sensible heat flux during HWDs is much larger over forest than over grassland. In the long term, however, elevated evaporative cooling expedites soil moisture depletion, and grassland rather than forest becomes the main heat source. The regional climate system then shifts to a new regime characterized by a larger heating and even higher temperatures, such as during the catastrophic 2003 heatwave in France. By focusing strictly on the event timescale we could identify patterns that did not emerge in previous analyses on longer timescales<sup>9,10,14</sup>. Our results also highlight the dual role of forest in the terrestrial energy and water budgets: on the one hand the conservative character of forest ET (refs 21,28) accommodates higher sensible heat fluxes during HWDs, but on the other hand low losses are beneficial for water resources and prevent heatwave amplification in the long run. Such tradeoffs will become increasingly important in a warming climate.

## Methods

**HWD definition.** The World Meteorological Organization defines a HWD as a day in a sequence of at least five days during which the daily maximum temperature exceeds the climatological mean over the reference period 1961–1990 by at least 5 K. In this study we adopt this definition but determine the climatology on the basis of the available data in the period 1997–2008. As a result of the increasing temperature trend in Europe, our method will generally result in fewer HWDs.

**Flux measurements.** Concomitant observations of land surface radiation, energy and water budget components come from the La Thuile FLUXNET synthesis data set (www.fluxdata.org). This data set provides direct and continuous eddy covariance flux measurements for over 170 sites across different climate and vegetation zones. For this study, only data from sites within the temperate climate zone of central-western Europe and with at least two (for climatology) or three (for anomalies) years of data were used. Gap-filled data and days with rain between 9:00 and 13:00 UTC were omitted from the analysis. In the analysis we distinguished between forested sites and sites with short (perennial) vegetation. Grassland and cropland sites were found to respond similarly to heatwave conditions.

**Temperature measurements.** Station data shown in Fig. 5 were taken from the European Climate Analysis and Dataset (eca.knmi.nl).

**Satellite data.** Daily quality-screened MODIS collection 5 LST at 1 km (MOD11A1 from TERRA and MYD11A1 from AQUA) were regridded to 0.1° using the following procedure: (1) pixels with cloud, aerosol or cloud shadow artefacts (screening by QA bits 0 and 1) were excluded; (2) weighted averaging to a 0.1° regular grid was carried out by weighting by the inverse of the LST error (evaluation of QA bits 6 and 7). The resulting spatiotemporal composite includes the 10–25% most reliable clear-sky pixels for the given area with four daily time steps. MODIS LST anomalies were calculated with respect to cloud-free conditions over a 15-day period centred on the day of interest for the years 2000–2008 (Terra) or 2003–2008 (Aqua) but excluding 2003 and July 2006.

**Anomaly calculation.** When studying climate variability, it is useful to isolate the dynamic effects in a variable X from those imposed by the mean seasonal cycle:  $\Delta X = X - X_{\text{clim}}$ . The uncertainty associated with the anomaly  $\Delta X$  can be written as:  $\sigma_{\Delta X}^2 = \sigma_X^2 + \sigma_{X_{\text{clim}}}^2 - 2\rho\sigma_X\sigma_{X_{\text{clim}}}$ . When  $\Delta X$  can be estimated from all data within the defined climatology period (that is, no gaps),  $\sigma_X^2$  will dominate  $\sigma_{\Delta X}^2$ . On the other hand, when estimating  $X_{\text{clim}}$  from a sample of the whole population, then  $\sigma_{X_{\text{clim}}}^2 \gg \sigma_X^2$  and to a good approximation  $\sigma_{\Delta X}^2 \approx \sigma_{X_{\text{clim}}}^2$ . We investigate the potential for estimating  $\Delta X$  from a limited sample of the whole population by applying a random combination method on gapless data (see Supplementary Fig. S4). This is relevant because different sites have different temporal coverage, and no single year can be defined as a reference for all sites. Here we find that using at least 2 years of data and a 15-day window reduces  $\sigma_{\Delta X}^2$  sufficiently for practical applications.

**Conceptual drydown model.** Key changes in the land surface energy budget during heatwaves are driven by changes in soil moisture. A three-step model describes the impact of soil moisture on the sensible heat flux evolution. First we construct conceptual curves that relate storage and ET. The levels of the curves during stage I drying (with no sensitivity to soil moisture storage depletion S) correspond to the median values listed in Fig. 1 for the climatology (thin dashed lines in Fig. 4) and climatology plus HWD anomaly (thick lines). During stage II drying, ET becomes self-limiting and decays approximately exponentially<sup>29,44</sup>. The curves during stage II and III drying are constructed to be consistent with independent observations showing that (1) forest ecosystems have deeper roots<sup>27,45,46</sup> (25% deeper<sup>45</sup>) and (2) ET decays faster over grassland<sup>29,31</sup>. The conversion from the curves in Fig. 3a,b is done using a simplified water budget without drainage and precipitation input, that is,  $dS/dt = ET$  with a conversion between midday and daily ET of 0.3. Finally, the conversion from the curves in Fig. 4b,c is done by assuming no change in available energy, that is,  $\lambda ET + H = \text{constant}$ .

Received 26 April 2010; accepted 3 August 2010; published online 5 September 2010

## References

- Schär, C. *et al.* The role of increasing temperature variability for European summer heatwaves. *Nature* **427**, 332–336 (2004).
- Seneviratne, S. I., Lüthi, D., Litschi, M. & Schär, C. Land–atmosphere coupling and climate change in Europe. *Nature* **443**, 205–209 (2006).
- Fischer, E. M. & Schär, C. Consistent geographical patterns of changes in high-impact European heatwaves. *Nature Geosci.* **3**, 398–403 (2010).
- Beniston, M. The 2003 heat wave in Europe: A shape of things to come? An analysis based on Swiss climatological data and model simulations. *Geophys. Res. Lett.* **31**, L02202 (2004).
- Della-Marta, P. M., Haylock, M. R., Luterbacher, J. & Wanner, H. Doubled length of western European summer heat waves since 1880. *J. Geophys. Res.* **112**, D15103 (2007).
- Black, E. *et al.* Factors contributing to the summer 2003 European heatwave. *Weather* **59**, 217–223 (2004).
- García-Herrera, R. *et al.* A review of the European summer heatwave of 2003. *Crit. Rev. Environ. Sci. Technol.* **40**, 267–306 (2010).
- Zaitchik, B. F., Macalady, A. K., Bonneau, L. R. & Smith, R. B. Europe's 2003 heat wave: A satellite view of impacts and land–atmosphere feedbacks. *Int. J. Climatol.* **26**, 743–769 (2006).
- Rebetez, M., Dupont, O. & Giroud, M. An analysis of the July 2006 heatwave extent in Europe compared to the record year of 2003. *Theor. Appl. Climatol.* **95**, 1–9 (2009).
- Ciais, P. *et al.* Europe-wide reduction in primary productivity caused by the heat and drought in 2003. *Science* **437**, 529–533 (2005).
- Fischer, E. M., Seneviratne, S. I., Lüthi, D. & Schär, C. Contribution of land–atmosphere coupling to recent European summer heat waves. *Geophys. Res. Lett.* **34**, L06707 (2007).
- Fouillet, A. *et al.* Has the impact of heat waves on mortality changed in France since the European heat wave of summer 2003? A study of the 2006 heat wave. *Int. J. Epidemiol.* **37**, 309–317 (2008).
- Cassou, C., Terray, L. & Phillips, A. S. Tropical Atlantic influence on European heat waves. *J. Clim.* **18**, 2805–2811 (2005).
- Ferranti, F. & Viterbo, P. The European summer of 2003: Sensitivity to soil water initial conditions. *J. Clim.* **19**, 3659–3680 (2006).

15. Shukla, J., Nobre, C. & Sellers, P. Amazon deforestation and climate change. *Science* **247**, 1322–1325 (1990).
16. Wang, J. *et al.* Impact of deforestation in the Amazon basin on cloud climatology. *Proc. Natl Acad. Sci. USA* **106**, 3670–3674 (2009).
17. Bonan, G. B. Forests and climate change: Forcings, feedbacks, and the climate benefits of forests. *Science* **320**, 1444–1449 (2008).
18. Pitman, A. J. *et al.* Uncertainties in climate responses to past land cover change: First results from the LUCID intercomparison study. *Geophys. Res. Lett.* **36**, L14814 (2009).
19. Jackson, R. B. *et al.* Protecting climate with forests. *Environ. Res. Lett.* **3**, 044006 (2008).
20. Anderson, R. G. *et al.* Biophysical considerations in forestry for climate protection. *Front. Ecol. Environ.* doi:10.1890/090179 (2010).
21. Shuttleworth, J. W. & Calder, I. R. Has the Priestley–Taylor equation any relevance to forest evaporation? *J. Appl. Meteorol.* **18**, 639–646 (1979).
22. Zhang, L., Dawes, W. R. & Walker, G. R. Response of mean annual evapotranspiration to vegetation changes at catchment scale. *Wat. Resour. Res.* **37**, 701–708 (2001).
23. Hetherington, A. M. & Woodward, F. I. The role of stomata in sensing and driving environmental change. *Nature* **424**, 901–908 (2003).
24. Kelliher, F. M., Leuning, R. & Schulze, E. D. Evaporation and canopy characteristics of coniferous forests and grasslands. *Oecologia* **95**, 153–163 (1993).
25. Jarvis, P. G. & McNaughton, K. G. Stomatal control of transpiration—scaling up from leaf to region. *Adv. Ecol. Res.* **15**, 1–49 (1986).
26. Granier, A., Biron, P. & Lemoine, D. Water balance, transpiration and canopy conductance in two beech stands. *Agric. Forest Meteorol.* **100**, 291–308 (2000).
27. Schenk, H. J. & Jackson, R. B. The global biogeography of roots. *Ecol. Monogr.* **72**, 311–328 (2002).
28. Roberts, J. Forest transpiration: A conservative hydrological process? *J. Hydrol.* **66**, 133–141 (1983).
29. Teuling, A. J., Seneviratne, S. I., Williams, C. & Troch, P. A. Observed timescales of evapotranspiration response to soil moisture. *Geophys. Res. Lett.* **33**, L23403 (2006).
30. Wicke, W. & Bernhofer, C. Energy balance comparison of the Hartheim forest and an adjacent grassland site during the HartX experiment. *Theor. Appl. Climatol.* **53**, 49–58 (1996).
31. Baldocchi, D. D., Xu, L. K. & Kiang, N. How plant functional-type, weather, seasonal drought, and soil physical properties alter water and energy fluxes of an oak-grass savanna and an annual grassland. *Agric. Forest Meteorol.* **123**, 13–39 (2004).
32. von Randow, C. *et al.* Comparative measurements and seasonal variations in energy and carbon exchange over forest and pasture in South West Amazonia. *Theor. Appl. Climatol.* **78**, 5–26 (2004).
33. Baldocchi, D. *et al.* FLUXNET: A new tool to study the temporal and spatial variability of ecosystem-scale carbon dioxide, water vapor, and energy flux densities. *Bull. Am. Meteorol. Soc.* **82**, 2415–2434 (2001).
34. Wilson, K. B. *et al.* Energy balance closure at FLUXNET sites. *Agric. Forest Meteorol.* **113**, 223–243 (2002).
35. Moderow, U. *et al.* Available energy and energy balance closure at four coniferous forest sites across Europe. *Theor. Appl. Climatol.* **98**, 397–412 (2009).
36. Ibrom, A. *et al.* Strong low-pass filtering effects on water vapour flux measurements with closed-path eddy correlation systems. *Agric. Forest Meteorol.* **147**, 140–156 (2007).
37. Foken, T. *et al.* Some aspects of the energy balance closure problem. *Atmos. Chem. Phys.* **6**, 4395–4402 (2006).
38. Gash, J. H. C. & Dolman, A. J. Sonic anemometer (co)sine response and flux measurement I. The potential for (co)sine error to affect sonic anemometer-based flux measurements. *Agric. Forest Meteorol.* **119**, 195–207 (2003).
39. Lindroth, A., Mölder, M. & Lagergren, F. Heat storage in forest biomass improves energy balance closure. *Biogeosciences* **7**, 301–313 (2010).
40. van der Molen, M. K., Gash, J. H. C. & Elbers, J. A. Sonic anemometer (co)sine response and flux measurement II. The effect of introducing an angle of attack dependent calibration. *Agric. Forest Meteorol.* **122**, 95–109 (2004).
41. Teuling, A. J. & Seneviratne, S. I. Contrasting spectral changes limit albedo impact on land–atmosphere coupling during the 2003 European heat wave. *Geophys. Res. Lett.* **35**, L03401 (2008).
42. Teuling, A. J., Uijlenhoet, R., Hupet, F. & Troch, P. A. Impact of plant water uptake strategy on soil moisture and evapotranspiration dynamics during drydown. *Geophys. Res. Lett.* **33**, L03401 (2006).
43. Seneviratne, S. I. *et al.* Investigating soil moisture–climate interactions in a changing climate: A review. *Earth Sci. Rev.* **99**, 125–161 (2010).
44. Brutsaert, W. & Chen, D. Desorption and the two stages of drying of natural tallgrass prairie. *Wat. Resour. Res.* **31**, 1305–1313 (1995).
45. Zeng, X. Global vegetation root distribution for land modeling. *J. Hydrometeorol.* **2**, 525–530 (2001).
46. Breuer, L., Eckhardt, K. & Frede, H.-G. Plant parameter values for models in temperate climates. *Ecol. Model.* **169**, 237–293 (2003).
47. Juang, J.-Y. *et al.* Separating the effects of albedo from eco-physiological changes on surface temperature along a successional chronosequence in the southeastern United States. *Geophys. Res. Lett.* **34**, L21408 (2007).
48. Andersen, O. B., Seneviratne, S. I., Hinderer, J. & Viterbo, P. GRACE-derived terrestrial water storage depletion associated with the 2003 European heat wave. *Geophys. Res. Lett.* **32**, L18405 (2005).
49. Wilson, K. B. *et al.* Energy partitioning between latent and sensible heat flux during the warm season at FLUXNET sites. *Wat. Resour. Res.* **38**, 1294 (2002).
50. Seitz, F., Schmidt, M. & Shum, C. K. Signals of extreme weather conditions in Central Europe in GRACE 4-D hydrological mass variations. *Earth Planet. Sci. Lett.* **268**, 165–170 (2008).

## Acknowledgements

We are grateful to the members of the FLUXNET community (<http://www.fluxdata.org/DataInfo/default.aspx>) and in particular the CarboEuropeIP network for their efforts in acquiring the eddy covariance data. We acknowledge the financial support to the eddy covariance data harmonization provided by CarboEuropeIP, FAO-GTOS-TCO, iLEAPS, Max Planck Institute for Biogeochemistry, National Science Foundation, University of Tuscia, Université Laval and Environment Canada and US Department of Energy and the database development and technical support from Berkeley Water Center, Lawrence Berkeley National Laboratory, Microsoft Research eScience, Oak Ridge National Laboratory, University of California - Berkeley and University of Virginia. A.J.T. acknowledges financial support from Netherlands Organisation for Scientific Research (NWO) through Rubicon grant 825.07.009, ETH Zurich and the Swiss National Science Foundation through the NFP61 DROUGHT-CH project. We further acknowledge support from the European Commission Project CARBO-Extreme (FP7-ENV-2008-1-226701), the CCES MAIOLICA project and NCCR-Climat programme.

## Author contributions

A.J.T. and S.I.S. provided the framework and conceived the manuscript. A.J.T. carried out all analyses. All authors collaborated in the discussion of the results and writing.

## Additional information

The authors declare no competing financial interests. Supplementary information accompanies this paper on [www.nature.com/naturegeoscience](http://www.nature.com/naturegeoscience). Reprints and permissions information is available online at <http://npg.nature.com/reprintsandpermissions>. Correspondence and requests for materials should be addressed to A.J.T. or S.I.S.